

Extracting quantum-geometric effects from Ginzburg-Landau theory in a multiband Hubbard model

M. Iskin¹

¹*Department of Physics, Koç University, Rumelifeneri Yolu, 34450 Sarıyer, İstanbul, Türkiye*
(Dated: June 6, 2023)

We first apply functional-integral approach to a multiband Hubbard model near the critical pairing temperature, and derive a generic effective action that is quartic in the fluctuations of the pairing order parameter. Then we consider time-reversal-symmetric systems with uniform (i.e., at both low-momentum and low-frequency) pairing fluctuations in a unit cell, and derive the corresponding time-dependent Ginzburg-Landau (TDGL) equation. In addition to the conventional intraband contribution that depends on the derivatives of the Bloch bands, we show that the kinetic coefficients of the TDGL equation have a geometric contribution that is controlled by both the quantum-metric tensor of the underlying Bloch states and their band-resolved quantum-metric tensors. Furthermore we show that thermodynamic properties such as London penetration depth, GL coherence length, GL parameter and upper critical magnetic field have an explicit dependence on quantum geometry.

I. INTRODUCTION

In modern solid-state and condensed-matter systems, the Berry curvature tensor and quantum-metric tensor play vital roles in characterizing the quantum topology and geometry of the underlying Bloch states [1–3]. The Berry curvature, in particular, is crucial in calculating the Chern number, which is a topological invariant that quantifies the ‘magnetic charge’ of occupied electronic bands in a crystal. This number determines the transport properties of some materials, and provides a robust way to classify and characterize the topological phases of matter [4, 5]. Another useful tool is the quantum metric, which has broad applications across various fields of physics, including superconductivity in multi-band materials [6–10]. It is especially significant in explaining how an isolated flat band can carry finite superfluid current [11].

Assuming weak interactions, time-reversal symmetry, and uniform pairing, it is possible to show that the quantum metric of the isolated flat band exclusively describes the superfluid density, allowing superconductivity to prevail [12–14]. Interestingly, despite the diverging band mass of its unpaired constituents and the smallness of onsite attractive interaction between particles, a Cooper pair can still acquire a finite effective mass through virtual interband transitions in the form of quantum metric. In addition, by solving the two-body problem in a multiband lattice [15–17], the geometric origin of superfluid density can be traced all the way back to the effective mass of the lowest-lying bound states through an exact calculation [16, 17]. Since the effective mass of Cooper pairs can be attributed to the geometric origin of superfluid density [18–21], the low-energy collective modes (i.e., Goldstone and Leggett modes) are again influenced by the quantum metric in a similar way [22, 23]. These peculiar findings highlight the essence of the role played by quantum metric in flat-band superconductivity, and they may offer a fresh perspective for the theory of multiband superconductors [11, 20, 21, 24].

In this paper, to gain further insight into the thermodynamic properties of multiband superconductors, we begin with a generic multiband Hubbard model and derive its effective quartic action in the fluctuations of the pairing order parameter near the critical transition temperature. Then we focus on the simpler problem, and assume that the system exhibits time-reversal symmetry and uniform pairing fluctuations. We demonstrate that the kinetic coefficients of the resulting time-dependent Ginzburg-Landau (TDGL) equation have a geometric interband contribution that is controlled by both the quantum-metric tensor of the underlying Bloch states and their band-resolved quantum-metric tensors. Finally, we extract the effective mass of the Cooper pairs, London penetration depth, GL coherence length, GL parameter, upper critical magnetic field, superfluid density and BKT transition temperature as examples of thermodynamic properties that depend explicitly on quantum geometry through a standard GL analysis.

The rest of the paper is organized as follows. In Sec. II we apply functional-integral approach to the multiband Hubbard model, and derive a generic effective action that is quartic in the fluctuations of the pairing order parameter. In Sec. III we specifically consider time-reversal-symmetric systems with uniform pairing fluctuations, and derive and analyze the resultant TDGL equation. The paper ends with a brief summary of our conclusions and an outlook in Sec. IV.

II. FUNCTIONAL-INTEGRAL FORMALISM

In this Section we apply imaginary-time functional path-integral approach to a generic multiband Hubbard model near the critical pairing temperature T_c , and derive an effective action that is quartic in the fluctuations of the pairing order parameter [25, 26].

A. Multiband Hubbard model

Our starting Hamiltonian for a multiband Hubbard model is $\mathcal{H} = -\sum_{SS'ii'\sigma} t_{Si,S'i'}^\sigma \psi_{Si\sigma}^\dagger \psi_{S'i'\sigma} - \sum_{S\sigma} \mu_\sigma \psi_{Si\sigma}^\dagger \psi_{Si\sigma} - U \sum_{Si} \psi_{Si\uparrow}^\dagger \psi_{Si\downarrow}^\dagger \psi_{Si\downarrow} \psi_{Si\uparrow}$, where i denotes a particular unit cell in the lattice and S denotes its sublattice sites in such a way that $t_{Si,S'i'}^\sigma$ corresponds to the hopping parameter from a site $S' \in i'$ to a site $S \in i$, and μ_σ is the chemical potential that fixes the number of spin- σ particles. Thus while the kinetic energy term is quite generic, for simplicity we consider only attractive onsite interactions (i.e., $U \geq 0$) between \uparrow and \downarrow particles. Then we express the Hubbard Hamiltonian in reciprocal space through a canonical transformation $\psi_{Si\sigma}^\dagger = \frac{1}{\sqrt{N_c}} \sum_{\mathbf{k}} e^{-i\mathbf{k}\cdot\mathbf{r}_{Si}} \psi_{S\mathbf{k}\sigma}^\dagger$, where N_c is the number of unit cells in the lattice, \mathbf{k} is the crystal momentum in the first Brillouin zone, and \mathbf{r}_{Si} is the position of site $S \in i$. The total number of lattice sites is $N_c N_S$ where N_S is the number of sublattice sites in a unit cell. This leads to

$$\mathcal{H} = \sum_{SS'\mathbf{k}\sigma} \psi_{S\mathbf{k}\sigma}^\dagger [h_{SS'}^\sigma(\mathbf{k}) - \mu_\sigma \delta_{SS'}] \psi_{S'\mathbf{k}\sigma} - U \sum_{S\mathbf{k}\mathbf{k}'\mathbf{q}} \psi_{S\mathbf{k}\uparrow}^\dagger \psi_{S,-\mathbf{k}+\mathbf{q},\downarrow}^\dagger \psi_{S,-\mathbf{k}+\mathbf{q},\downarrow} \psi_{S\mathbf{k}'\uparrow}, \quad (1)$$

where $h_{SS'}^\sigma(\mathbf{k})$ is the matrix element of the Bloch Hamiltonian in the sublattice basis, and \mathbf{q} is the center-of-mass momentum of the incoming and outgoing pair of particles. Except for Sec. III C, we work in units of $\hbar \rightarrow 1$ the Planck constant.

B. Effective quartic action near T_c

In the Grassmann functional-integral formalism [25, 26], the grand partition function $\mathcal{Z} = \text{Tre}^{-\beta\mathcal{H}}$, can be written as $\mathcal{Z} = \int \mathcal{D}[\psi^\dagger, \psi] e^{-\mathcal{S}}$, where \mathcal{S} is the associated fermionic action given by $\mathcal{S} = \int_0^\beta d\tau [\sum_{S\mathbf{k}\sigma} \psi_{S\mathbf{k}\sigma}^\dagger(\tau) \partial_\tau \psi_{S\mathbf{k}\sigma}(\tau) + \mathcal{H}(\tau)]$. Here τ is the imaginary time, and $\beta = 1/(k_B T)$ is the inverse temperature in units of $k_B \rightarrow 1$ the Boltzmann constant. By first introducing the usual Hubbard-Stratanovich transformation that linearizes the interaction term at the expense of introducing a complex bosonic field $\Delta_S(q)$, and then integrating out the remaining fermionic degrees of freedom that is Gaussian in the Grassmann fields, we eventually obtain $\mathcal{Z} = \int \mathcal{D}[\Delta^*, \Delta] e^{-\mathcal{S}_{\text{eff}}}$. Here $\Delta_S(q)$ corresponds to the pairing order parameter, and

$$\mathcal{S}_{\text{eff}} = \beta \sum_q \frac{|\Delta_S(q)|^2}{U} + \frac{\beta}{N_c} \sum_{S\mathbf{k}} [h_{SS}^\downarrow(\mathbf{k}) - \mu_\downarrow] - \frac{1}{N_c} \text{Tr} \sum_{kq} \ln[\beta \mathbf{G}^{-1}(k, q)] \quad (2)$$

is an effective bosonic action for the resultant pairs, where we make use of the well-known identity $\ln \det \mathbf{M} =$

$\text{Tr} \ln \mathbf{M}$ with Tr denoting a trace over the sublattice and particle-hole sectors, and the $2N_S \times 2N_S$ matrix $\mathbf{G}^{-1}(k, q)$ denoting the inverse propagator. Throughout this paper, we use the collective indices $q \equiv (\mathbf{q}, i\nu_\ell)$ and $k \equiv (\mathbf{k}, i\omega_\ell)$, where $\nu_\ell = 2\ell\pi/\beta$ is the bosonic Matsubara frequency and $\omega_\ell = (2\ell + 1)\pi/\beta$ is the fermionic one.

In order to make analytical progress with this action, we first decompose $\Delta_S(q) = \Delta_S \delta_{q0} + \Lambda_S(q)$ in terms of a q -independent (i.e., stationary) saddle-point parameter Δ_S and a q -dependent fluctuations around it, and split the inverse propagator

$$\mathbf{G}^{-1}(k, q) = \mathbf{G}_0^{-1}(k) + \mathbf{\Sigma}(q) \quad (3)$$

into two, where $\mathbf{G}_0^{-1}(k)$ depends on Δ_S and $\mathbf{\Sigma}(q)$ depends solely on $\Lambda_S(q)$. Here δ_{ij} is a Kronecker delta. Then we reexpress the inverse propagator as $\mathbf{G}_0^{-1}(k) [\mathcal{I}_{2N_S} + \mathbf{G}_0(k) \mathbf{\Sigma}(q)]$ and expand its natural logarithm as a Taylor series in $\Lambda_S(q)$, leading to $\ln[\beta \mathbf{G}^{-1}(k, q)] = \ln[\beta \mathbf{G}_0^{-1}(k)] - \sum_{j=1}^{\infty} \frac{(-1)^j}{j} [\mathbf{G}_0(k) \mathbf{\Sigma}(q)]^j$. In this paper we set $\Delta_S \rightarrow 0$ since we are only interested in the normal state properties near the critical pairing temperature when $T \rightarrow T_c$. This particular limit allows us to go beyond the trivial saddle-point action $\mathcal{S}_0 = \frac{\beta}{N_c} \sum_{S\mathbf{k}} [h_{SS}^\downarrow(\mathbf{k}) - \mu] - \frac{1}{N_c} \sum_{\mathbf{k}} \ln \det[\beta \mathbf{G}_0^{-1}(k)]$, and calculate both the quadratic action \mathcal{S}_2 and the quartic action \mathcal{S}_4 . The resultant effective action $\mathcal{S}_{\text{eff}} \approx \mathcal{S}_0 + \mathcal{S}_2 + \mathcal{S}_4$ is expected to be qualitatively accurate in describing the low-energy physics at all coupling strengths.

When the saddle-point order parameter $\Delta_S \rightarrow 0$ is trivial, the saddle-point component of the inverse propagator $\mathbf{G}_0^{-1}(k) = \begin{bmatrix} (\mathbf{G}_0^{11})^{-1}(k) & 0 \\ 0 & (\mathbf{G}_0^{22})^{-1}(k) \end{bmatrix}$ becomes diagonal in the particle-hole sector, where its matrix element $(G_0^{11})_{SS'}^{-1}(k) = (i\omega_\ell + \mu_\uparrow) \delta_{SS'} - h_{SS'}^\uparrow(\mathbf{k})$ describes a spin- \uparrow particle in the sublattice sector. Similarly $(G_0^{22})_{SS'}^{-1}(k) = (i\omega_\ell - \mu_\downarrow) \delta_{SS'} + h_{SS'}^{\downarrow*}(-\mathbf{k})$ describes a spin- \downarrow hole. On the other hand the fluctuation component $\mathbf{\Sigma}(q) = \begin{bmatrix} 0 & \mathbf{\Sigma}^{12}(q) \\ \mathbf{\Sigma}^{21}(q) & 0 \end{bmatrix}$ is off-diagonal in the particle-hole sector by definition, where $\Sigma_{SS'}^{12}(q) = \Lambda_S(q) \delta_{SS'}$ and $\Sigma_{SS'}^{21}(q) = \Lambda_S^*(-q) \delta_{SS'}$ are diagonal in the sublattice sector due to the onsite interactions considered in this paper. For convenience we represent the matrix elements of the non-interacting propagators $\mathbf{G}_0^{11}(k)$ and $\mathbf{G}_0^{22}(k)$ as

$$G_{SS'}^{11}(k) = \sum_n \frac{n_{S\mathbf{k}\uparrow} n_{S'\mathbf{k}\uparrow}^*}{i\omega_\ell - \xi_{n\mathbf{k}\uparrow}}, \quad (4)$$

$$G_{SS'}^{22}(k) = \sum_n \frac{n_{S,-\mathbf{k},\downarrow}^* n_{S',-\mathbf{k},\downarrow}}{i\omega_\ell + \xi_{n,-\mathbf{k},\downarrow}}, \quad (5)$$

where $n_{S\mathbf{k}\sigma} = \langle S | n_{\mathbf{k}\sigma} \rangle$ is the projection of the periodic part of the Bloch state onto sublattice S , and $\xi_{n\mathbf{k}\sigma} = \varepsilon_{n\mathbf{k}\sigma} - \mu_\sigma$ is associated with the corresponding Bloch band $\varepsilon_{n\mathbf{k}\sigma}$. They are in such a way that

$\sum_{S'} h_{SS'}^\sigma(\mathbf{k}) n_{S'\mathbf{k}\sigma} = \varepsilon_{n\mathbf{k}\sigma} n_{S\mathbf{k}\sigma}$, and the propagators satisfy $\mathbf{G}_0^{11}(k)(\mathbf{G}_0^{11})^{-1}(k) = \mathcal{I}_{N_S}$ and $\mathbf{G}_0^{22}(k)(\mathbf{G}_0^{22})^{-1}(k) = \mathcal{I}_{N_S}$, where \mathcal{I}_{N_S} is an $N_S \times N_S$ identity matrix.

Using Eqs. (4) and (5) in the quadratic action $\mathcal{S}_2 = \frac{\beta}{U} \sum_{S'q} |\Lambda_{S'}(q)|^2 + \frac{1}{2N_c} \text{Tr} \sum_{kq} \mathbf{G}_0(k) \boldsymbol{\Sigma}(q) \mathbf{G}_0(k-q) \boldsymbol{\Sigma}(-q)$, and after evaluating the trace, we obtain

$$\mathcal{S}_2 = \beta \sum_{SS'q} \Lambda_S^*(q) \Gamma_{SS'}^{-1}(q) \Lambda_{S'}(q), \quad (6)$$

where $\Gamma_{SS'}^{-1}(q) = \delta_{SS'}/U + \frac{1}{\beta N_c} \sum_k G_{SS'}^{11}(k) G_{S'S}^{22}(k-q)$ is the matrix element of the inverse pair fluctuation propagator $\Gamma^{-1}(q)$. The corresponding Feynman diagram is sketched in Fig. 1(i). By evaluating the Matsubara summation over ω_ℓ , we find

$$\Gamma_{SS'}^{-1}(q) = \frac{\delta_{SS'}}{U} + \frac{1}{2N_c} \sum_{nm\mathbf{k}} \frac{\mathcal{X}_{n\mathbf{k}\uparrow} + \mathcal{X}_{m,-\mathbf{k}+\mathbf{q},\downarrow}}{i\nu_\ell - \xi_{n\mathbf{k}\uparrow} - \xi_{m,-\mathbf{k}+\mathbf{q},\downarrow}} \times n_{S\mathbf{k}\uparrow} n_{S'\mathbf{k}\uparrow}^* m_{S',-\mathbf{k}+\mathbf{q},\downarrow}^* m_{S,-\mathbf{k}+\mathbf{q},\downarrow}, \quad (7)$$

where $\mathcal{X}_{n\mathbf{k}\sigma} = \tanh(\beta\xi_{n\mathbf{k}\sigma}/2) = 1 - 2f(\xi_{n\mathbf{k}\sigma})$ is the usual thermal factor with $f(\varepsilon) = 1/(e^{\beta\varepsilon} + 1)$ the Fermi-Dirac distribution.

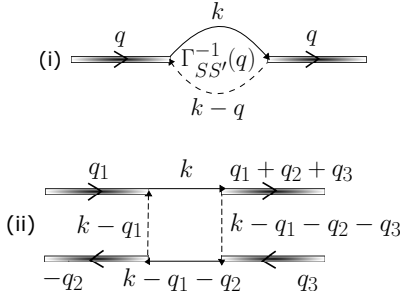


FIG. 1. Diagrammatic representation of the fluctuation contributions that give rise to (i) quadratic action and (ii) quartic action. While the pair propagators are shown as colored bars, the particle and hole propagators are shown as solid and dashed lines, respectively.

There are two important remarks about Eq. (7). First we note that the generalized Thouless condition

$$b_{SS'S''S'''}(0,0,0) = \frac{1}{2N_c} \sum_{n_1 n_2 n_3 n_4 \mathbf{k}} \frac{n_{1S\mathbf{k}\uparrow} n_{1S'\mathbf{k}\uparrow}^* n_{2S',-\mathbf{k},\downarrow} n_{2S'',-\mathbf{k},\downarrow} n_{3S''\mathbf{k}\uparrow} n_{3S'''\mathbf{k}\uparrow}^* n_{4S''',-\mathbf{k},\downarrow} n_{4S,-\mathbf{k},\downarrow}}{(\xi_{n_1\mathbf{k}\uparrow} + \xi_{n_2,-\mathbf{k},\downarrow})(\xi_{n_3\mathbf{k}\uparrow} + \xi_{n_4,-\mathbf{k},\downarrow})} \times \left[\frac{\mathcal{X}_{n_1\mathbf{k}\uparrow} + \mathcal{X}_{n_4,-\mathbf{k},\downarrow}}{\xi_{n_1\mathbf{k}\uparrow} + \xi_{n_4,-\mathbf{k},\downarrow}} + \frac{\mathcal{X}_{n_3\mathbf{k}\uparrow} + \mathcal{X}_{n_2,-\mathbf{k},\downarrow}}{\xi_{n_3\mathbf{k}\uparrow} + \xi_{n_2,-\mathbf{k},\downarrow}} - \frac{\mathcal{X}_{n_1\mathbf{k}\uparrow} - \mathcal{X}_{n_3\mathbf{k}\uparrow}}{\xi_{n_1\mathbf{k}\uparrow} - \xi_{n_3\mathbf{k}\uparrow}} - \frac{\mathcal{X}_{n_2,-\mathbf{k},\downarrow} - \mathcal{X}_{n_4,-\mathbf{k},\downarrow}}{\xi_{n_2,-\mathbf{k},\downarrow} - \xi_{n_4,-\mathbf{k},\downarrow}} \right]. \quad (9)$$

As discussed in Sec. III C, this parameter characterizes the interactions between Cooper pairs. Note that a derivative is implied by the last two terms when the

$\det \Gamma^{-1}(\mathbf{0}, 0) = 0$ determines T_c in a multiband Hubbard model [27]. This is in such a way that $T_c = \max\{T_{c_1}, T_{c_2}, \dots, T_{c_{N_S}}\}$, where T_{c_j} is determined by setting the j th eigenvalue of $\Gamma^{-1}(\mathbf{0}, 0)$ to 0. In calculating T_c one needs to determine μ_σ self-consistently through the number equation $N_\sigma = -\partial\Omega/\partial\mu_\sigma \approx N_0^\sigma + N_2^\sigma$, where $\Omega = -\ln \mathcal{Z}/\beta$ is the grand potential. This leads to a saddle-point contribution $N_0^\sigma = \sum_{n\mathbf{k}} (1 - \mathcal{X}_{n\mathbf{k}\sigma})/2$ that originates from $\partial(\mathcal{S}_0/\beta)/\partial\mu_\sigma$ and a fluctuation contribution $N_2^\sigma = -\frac{1}{\beta} \sum_q \partial\{\ln \det[\Gamma^{-1}(q)/\beta]\}/\partial\mu_\sigma$ that is due to \mathcal{S}_2 after performing the Gaussian integration over the bosonic fluctuation fields. The saddle-point contribution by itself gradually fails to describe the low-energy physics with increasing coupling strengths, i.e., even at a qualitative level, and taking proper account of the fluctuation contribution is known to be a nontrivial yet crucial task in describing the strong-coupling limit [25, 28]. Second we are pleased to confirm that Eq. (7) and the associated Thouless condition are in perfect agreement with the self-consistency relation that determines the exact energy $E_{2b}(\mathbf{q})$ of the two-body bound states [16, 17], after setting the thermal factors $\mathcal{X}_{n\mathbf{k}\sigma} \rightarrow 1$ in $\Gamma^{-1}(\mathbf{q}, i\nu_\ell \rightarrow \omega + i0^+)$ together with the substitution $\omega + 2\mu \rightarrow E_{2b}(\mathbf{q})$.

Similarly, using Eqs. (4) and (5) in the quartic action $\mathcal{S}_4 = \frac{\beta}{4N_c} \text{Tr} \sum_{kq_1q_2q_3q_4} \mathbf{G}_0(k) \boldsymbol{\Sigma}(q_1) \mathbf{G}_0(k-q_1) \boldsymbol{\Sigma}(q_2) \mathbf{G}_0(k-q_1-q_2) \boldsymbol{\Sigma}(q_3) \mathbf{G}_0(k-q_1-q_2-q_3) \boldsymbol{\Sigma}(-q_1-q_2-q_3)$, and after evaluating the trace, we obtain

$$\mathcal{S}_4 = \frac{\beta}{2} \sum_{SS'S''S'''} b_{SS'S''S'''}(q_1, q_2, q_3) \Lambda_S^*(q_1 + q_2 + q_3) \times \Lambda_{S'}(q_1) \Lambda_{S''}^*(-q_2) \Lambda_{S'''}(q_3). \quad (8)$$

The corresponding Feynman diagram is sketched in Fig. 1(ii). While the q -dependence of the prefactor $b_{SS'S''S'''}(q_1, q_2, q_3) = \frac{1}{\beta N_c} \sum_k G_{SS'}^{11}(k) G_{S'S''}^{22}(k-q_1) G_{S''S'''}^{11}(k-q_1-q_2) G_{S''S}^{22}(k-q_1-q_2-q_3)$ is quite complicated in general, we approximate it with its stationary value at zero momentum and zero frequency (i.e., at $q_1 = q_2 = q_3 = 0$), which is a standard practice in basic BCS-BEC crossover theories [25, 26]. By evaluating the Matsubara summation over ω_ℓ , we find

summation indices n_1 and n_3 or similarly n_2 and n_4 refer to the same Bloch band, i.e., $d[\tanh(\beta\varepsilon/2)]/d\varepsilon = \frac{\beta}{2} \text{sech}^2(\beta\varepsilon/2)$. Thus Eqs. (6), (7), (8) and (9) all together

constitute our aforementioned action $\mathcal{S}_{\text{eff}} \approx \mathcal{S}_0 + \mathcal{S}_2 + \mathcal{S}_4$ near T_c for a generic multiband Hubbard model.

III. TIME-REVERSAL-SYMMETRIC SYSTEMS WITH UNIFORM PAIRING FLUCTUATIONS

In order to make further analytical progress, here we consider Hubbard models that manifest time-reversal symmetry, and set $n_{S,-\mathbf{k},\downarrow}^* = n_{S\mathbf{k}\uparrow} \equiv n_{S\mathbf{k}}$ and $\xi_{n,-\mathbf{k},\downarrow} = \xi_{n\mathbf{k}\uparrow} \equiv \xi_{n\mathbf{k}}$. Furthermore we limit our discussion to those systems where the low- q pairing fluctuations (i.e., at both low momentum and low frequency) are uniform in a unit cell, and set $\Lambda_S(q) = \Lambda_0(q)$ for all sublattices. For instance Mielke checkerboard and Kagome lattices may satisfy this condition because of their inversion symmetry as they satisfy the analogous condition in the two-body problem [16, 17]. The low-energy physics turns out to be very transparent in this particular limit as discussed next.

A. Effective quartic action

When both time-reversal-symmetry and uniform-pairing-fluctuation conditions met simultaneously, Eq. (6) can be written as $\mathcal{S}_2 = \beta \sum_q \Gamma_0^{-1}(q) |\Lambda_0(q)|^2$ and Eq. (8) can be written as $\mathcal{S}_4 = \frac{\beta b_0}{2} \sum_{q_1 q_2 q_3} \Lambda_0^*(q_1 + q_2 + q_3) \Lambda_0(q_1) \Lambda_0^*(-q_2) \Lambda_0(q_3)$. Using the completeness relation $\sum_S |S\mathbf{k}\rangle \langle S\mathbf{k}| = \mathcal{I}_{N_S}$ for the sublattice basis, Eqs. (7) and (9) reduce to

$$\Gamma_0^{-1}(q) = \frac{N_S}{U} + \frac{1}{2N_c} \sum_{nm\mathbf{k}} \frac{\mathcal{X}_{n\mathbf{k}} + \mathcal{X}_{m,\mathbf{k}-\mathbf{q}}}{i\nu_\ell - \xi_{n\mathbf{k}} - \xi_{m,\mathbf{k}-\mathbf{q}}} |\langle n_{\mathbf{k}} | m_{\mathbf{k}-\mathbf{q}} \rangle|^2, \quad (10)$$

$$b_0 = \frac{1}{N_c} \sum_{n\mathbf{k}} \left(\frac{\mathcal{X}_{n\mathbf{k}}}{4\xi_{n\mathbf{k}}^3} - \frac{\beta \mathcal{Y}_{n\mathbf{k}}}{8\xi_{n\mathbf{k}}^2} \right), \quad (11)$$

where $\mathcal{Y}_{n\mathbf{k}} = \text{sech}^2(\beta\xi_{n\mathbf{k}}/2)$ is another thermal factor. In the presence of a single band, Eqs. (10) and (11) recover the usual results [25, 26] after setting $N_S \rightarrow 1$ and $\langle n_{\mathbf{k}} | m_{\mathbf{k}-\mathbf{q}} \rangle \rightarrow \delta_{nm}$ since $n_{S\mathbf{k}} = 1$ is trivial for every \mathbf{k} state. Furthermore, in the presence of two bands, all of our results here and below are in full agreement with the recent literature on spin-orbit-coupled Fermi gases. There the helicity bands of a continuum model play exactly the same role as the Bloch bands of the lattice model as they also manifest time-reversal symmetry and naturally exhibit uniform pairing fluctuations in the spin sector [18, 19]. Next we show that the Bloch factor $|\langle n_{\mathbf{k}} | m_{\mathbf{k}-\mathbf{q}} \rangle|^2$ appearing in Eq. (10) is responsible for the appearance of quantum-geometric terms in the presence of two or more Bloch bands.

B. Low-momentum and low-frequency expansion

In the low-momentum regime, we expand the static part of the inverse pair propagator $\Gamma_0^{-1}(\mathbf{q}, 0) = a(T) + \frac{1}{2} \sum_{ij} c_{ij} q_i q_j + \dots$ as a Taylor series in \mathbf{q} [25, 26], and split the kinetic coefficient $c_{ij} = c_{ij}^{\text{intra}} + c_{ij}^{\text{inter}}$ into two contributions depending on whether the intraband or interband transition processes are involved. Here q_i refers to components of $\mathbf{q} = (q_x, q_y, q_z)$. A compact way to express the resultant expansion coefficients is

$$\begin{aligned} a(T) &= \frac{N_S}{U} - \frac{1}{N_c} \sum_{n\mathbf{k}} \frac{\mathcal{X}_{n\mathbf{k}}}{2\xi_{n\mathbf{k}}}, \quad (12) \\ c_{ij}^{\text{intra}} &= \frac{1}{N_c} \sum_{n\mathbf{k}} \left[\left(\frac{\mathcal{X}_{n\mathbf{k}}}{8\xi_{n\mathbf{k}}^2} - \frac{\beta \mathcal{Y}_{n\mathbf{k}}}{16\xi_{n\mathbf{k}}} \right) \ddot{\xi}_{n\mathbf{k}}^{ij} \right. \\ &\quad \left. + \beta^2 \frac{\mathcal{X}_{n\mathbf{k}} \mathcal{Y}_{n\mathbf{k}}}{16\xi_{n\mathbf{k}}} \dot{\xi}_{n\mathbf{k}}^i \dot{\xi}_{n\mathbf{k}}^j \right], \quad (13) \\ c_{ij}^{\text{inter}} &= \frac{1}{N_c} \sum_{n\mathbf{k}} \frac{\mathcal{X}_{n\mathbf{k}}}{2\xi_{n\mathbf{k}}} g_{ij}^{n\mathbf{k}} - \frac{1}{2N_c} \sum_{n \neq m, \mathbf{k}} \frac{\mathcal{X}_{n\mathbf{k}} + \mathcal{X}_{m\mathbf{k}}}{\xi_{n\mathbf{k}} + \xi_{m\mathbf{k}}} g_{ij}^{nm\mathbf{k}}, \quad (14) \end{aligned}$$

where the intraband contribution depends on the derivatives $\dot{\xi}_{n\mathbf{k}}^i \equiv \partial \xi_{n\mathbf{k}} / \partial k_i$ and $\ddot{\xi}_{n\mathbf{k}}^{ij} \equiv \partial^2 \xi_{n\mathbf{k}} / (\partial k_i \partial k_j)$ of the Bloch bands, and the interband contribution depends on the derivatives of the Bloch states through $g_{ij}^{n\mathbf{k}}$ and $g_{ij}^{nm\mathbf{k}}$ (defined further below). We note that the Thouless condition takes the usual form $a(T_c) = 0$, and determines T_c . For this reason we expand the zeroth-order coefficient as $a(T) = -a_0 \epsilon(T)$, where $a_0 = T_c [\partial a(T) / \partial T]_{T_c}$ and $\epsilon(T) = (1 - T/T_c)$. This leads to

$$a_0 = \frac{1}{2N_c} \sum_{n\mathbf{k}} \left[\frac{\mathcal{Y}_{n\mathbf{k}}}{2T_c} + \frac{\partial \mu}{\partial T} \left(\frac{\mathcal{Y}_{n\mathbf{k}}}{2\xi_{n\mathbf{k}}} - T_c \frac{\mathcal{X}_{n\mathbf{k}}}{\xi_{n\mathbf{k}}^2} \right) \right], \quad (15)$$

where the thermal factors are evaluated at T_c , and μ needs to be determined self-consistently via the number equation $\mathcal{N} = \sum_\sigma \mathcal{N}^\sigma \approx \mathcal{N}_0 + \mathcal{N}_2$. Here $\mathcal{N}_0 = \sum_{n\mathbf{k}} (1 - \mathcal{X}_{n\mathbf{k}})$ is the saddle-point contribution and $\mathcal{N}_2 = \frac{1}{\beta} \sum_q \partial \{ \ln[\beta \Gamma_0(q)] \} / \partial \mu$ comes from the fluctuations [25, 28].

The kinetic coefficient Eq. (13) is nothing but a summation over the usual single-band coefficient in disguise [19, 25]. This can be revealed by performing an integration by parts $\sum_{n\mathbf{k}} \mathcal{X}_{n\mathbf{k}} \dot{\xi}_{n\mathbf{k}}^i \dot{\xi}_{n\mathbf{k}}^j / \xi_{n\mathbf{k}}^3 = \beta \sum_{n\mathbf{k}} \mathcal{Y}_{n\mathbf{k}} \dot{\xi}_{n\mathbf{k}}^i \dot{\xi}_{n\mathbf{k}}^j / (4\xi_{n\mathbf{k}}^2) + \sum_{n\mathbf{k}} \mathcal{X}_{n\mathbf{k}} \ddot{\xi}_{n\mathbf{k}}^{ij} / (2\xi_{n\mathbf{k}}^2)$ that is followed by yet another integration by parts $\sum_{n\mathbf{k}} \mathcal{Y}_{n\mathbf{k}} \dot{\xi}_{n\mathbf{k}}^i \dot{\xi}_{n\mathbf{k}}^j / \xi_{n\mathbf{k}}^2 = -\beta \sum_{n\mathbf{k}} \mathcal{X}_{n\mathbf{k}} \mathcal{Y}_{n\mathbf{k}} \dot{\xi}_{n\mathbf{k}}^i \dot{\xi}_{n\mathbf{k}}^j / \xi_{n\mathbf{k}} + \sum_{n\mathbf{k}} \mathcal{Y}_{n\mathbf{k}} \ddot{\xi}_{n\mathbf{k}}^{ij} / \xi_{n\mathbf{k}}^2$ [29]. Thus c_{ij}^{intra} is precisely the so-called conventional contribution arising from the intraband processes. On the other hand the kinetic coefficient Eq. (14) depends on both the quantum-metric tensor $g_{ij}^{n\mathbf{k}}$ of the n th Bloch band and its band-resolved

quantum-metric tensor $g_{ij}^{nm\mathbf{k}}$ defined as

$$g_{ij}^{n\mathbf{k}} = 2\text{Re} \left[\langle \dot{n}_{\mathbf{k}}^i | (\mathcal{Z}_{N_s} - |n_{\mathbf{k}}\rangle \langle n_{\mathbf{k}}|) | \dot{n}_{\mathbf{k}}^j \rangle \right], \quad (16)$$

$$g_{ij}^{nm\mathbf{k}} = 2\text{Re} \left[\langle \dot{n}_{\mathbf{k}}^i | m_{\mathbf{k}} \rangle \langle m_{\mathbf{k}} | \dot{n}_{\mathbf{k}}^j \rangle \right], \quad (17)$$

where Re denotes the real part, $g_{ij}^{n\mathbf{k}} = \sum_{n \neq m} g_{ij}^{nm\mathbf{k}}$, and $|\dot{n}_{\mathbf{k}}^i\rangle \equiv \partial(|n_{\mathbf{k}}\rangle)/\partial k_i$. For this reason c_{ij}^{inter} is the so-called geometric contribution arising from the virtual interband processes [30]. The geometric terms appear only in a multiband Hubbard model, and their physical origin can be traced back to the Bloch factor appearing in Eq. (10). For instance, by expanding the Bloch state $|m_{\mathbf{k}-\mathbf{q}}\rangle = |m_{\mathbf{k}} - \sum_i \dot{n}_{\mathbf{k}}^i q_i + \frac{1}{2} \sum_{ij} \ddot{m}_{\mathbf{k}}^{ij} q_i q_j + \dots\rangle$ as a Taylor series in \mathbf{q} , one can easily show that $|\langle n_{\mathbf{k}} | m_{\mathbf{k}-\mathbf{q}} \rangle|^2 = \delta_{nm} - \frac{1}{2} \sum_{ij} [g_{ij}^{n\mathbf{k}} \delta_{nm} + g_{ij}^{nm\mathbf{k}} (\delta_{nm} - 1)] q_i q_j + \dots$ up to second-order in \mathbf{q} . Here the first derivative of the orthonormalization condition $\langle n_{\mathbf{k}} | m_{\mathbf{k}} \rangle = \delta_{nm}$ shows that the first-order coefficients vanish, where we also use its second derivative to obtain the final form.

In order to extract the low-frequency dependence of the inverse pair propagator, we expand $Q(i\nu_\ell) = \Gamma_0^{-1}(\mathbf{0}, i\nu_\ell) - \Gamma_0^{-1}(\mathbf{0}, 0)$ in powers of ω after the analytic continuation $i\nu_\ell \rightarrow \omega + i0^+$ [25]. Using the Cauchy principal value $1/(x \pm i0^+) = \mathcal{P}(1/x) \mp i\pi\delta(x)$, we expand $Q(\omega) = -d\omega + \dots$, and obtain $d = -\partial Q(\omega)/\partial \omega|_{\omega=0}$ as

$$d = \frac{1}{N_c} \sum_{n\mathbf{k}} \frac{\mathcal{X}_{n\mathbf{k}}}{4\xi_{n\mathbf{k}}^2} + \frac{i\pi\beta}{8N_c} \sum_n D_n(\mu)\theta_\mu. \quad (18)$$

Here $\delta(x)$ is the Dirac-delta distribution, $D_n(\varepsilon) = \sum_{\mathbf{k}} \delta(\varepsilon - \varepsilon_{n\mathbf{k}})$ is the density of states for the n th Bloch band, and $\theta_\varepsilon = \theta(\varepsilon - \min\{\varepsilon_{n\mathbf{k}}\})\theta(\max\{\varepsilon_{n\mathbf{k}}\} - \varepsilon)$ with $\theta(x)$ the Heaviside-step function. Thus the coefficient d has a positive imaginary part when μ lies within any one of the Bloch bands. Having derived the low-momentum and low-frequency expansion coefficients $a(T)$, b_0 , c_{ij} and d , we are ready to discuss the underlying GL theory and extract some quantum-geometric effects from it.

C. Ginzburg-Landau (GL) functional

For slowly-varying order parameter $\Lambda_0(x)$ in space and time near T_c , the TDGL equation

$$\left[a(T) + b_0 |\Lambda_0(x)|^2 - \sum_{ij} \frac{c_{ij}}{2} \nabla_i \nabla_j \right] \Lambda_0(x) = i\hbar d \frac{\partial \Lambda_0(x)}{\partial t} \quad (19)$$

is obtained by Fourier transforming the minimum action condition $\partial \mathcal{S}_{\text{eff}}/\partial \Lambda_0^*(x) = 0$ to real-space representation $x \equiv (\mathbf{x}, t)$, where ∇_i refers to the components of the gradient operator [25, 26]. Here b_0 , c_{ij} and d are evaluated at $T = T_c$. When the imaginary part of d is nonzero, e.g., in the weak coupling limit, this equation suggests that the dynamics of $\Lambda_0(x)$ is overdamped as a reflection of the

continuum of fermionic excitations into which a Cooper pair can decay. On the other hand $\Lambda_0(x)$ is propagating when d becomes purely real, e.g., in the strong-coupling limit away from half-filling. In the latter case one can scale the order parameter as $\Lambda_B(x) = \sqrt{d}\Lambda_0(x)$, and conclude that

$$(M_B^{-1})_{ij} = \frac{c_{ij}}{\hbar^2 d} \quad (20)$$

corresponds to the matrix elements of the inverse effective-mass tensor \mathbf{M}_B^{-1} of the Cooper pairs. Thus the quantum-metric tensor directly controls the inverse effective-mass tensor of the Cooper pairs [19]. In addition one also identifies $\mu_B(T) = -a(T)/d$ as the effective pair chemical potential and $U_{BB} = b_0/d^2$ as the effective pair-pair repulsion. We are pleased to confirm that the former conclusion coincides precisely with the inverse effective-mass tensor of the lowest-lying two-body bound states [16, 17], after setting the thermal factors $\mathcal{X}_{n\mathbf{k}} \rightarrow 1$ and $\mathcal{Y}_{n\mathbf{k}} \rightarrow 0$ together with the substitution $2\mu \rightarrow E_{2b}(\mathbf{0})$ in the remaining terms. Here $E_{2b}(\mathbf{0})$ is the energy of the lowest-lying two-body bound state at $\mathbf{q} = \mathbf{0}$, and its self-consistency relation coincides with the Thouless condition $a(T_c) = 0$ under the same settings [16, 17].

To study thermodynamic properties next we take a time-independent order parameter $\Lambda_0(x) \equiv \Lambda_0(\mathbf{x})$, and consider an isotropic kinetic coefficient $c_{ij} = c\delta_{ij}$ for its simplicity. Then we scale the order parameter as $\Psi(\mathbf{x}) = \sqrt{m_0 c/\hbar^2} \Lambda(\mathbf{x})$, and substitute $\nabla_i \rightarrow \nabla_i - 2iq_0 A_i/(\hbar c_0)$ to introduce an external magnetic field $\mathbf{H} = \nabla \times \mathbf{A}$, where q_0 is the charge of the particles, c_0 is the speed of light, m_0 is the mass of the particles, and $\mathbf{A}(\mathbf{x})$ is a slowly-varying vector potential. The resultant free-energy density has the standard GL form [26, 31, 32]

$$\begin{aligned} \mathcal{F}_{\text{GL}} = \mathcal{F}_n + \alpha(T) |\Psi|^2 + \frac{1}{2m_0} \left| \left(-i\hbar \nabla - \frac{2q_0}{c_0} \mathbf{A} \right) \Psi \right|^2 \\ + \frac{\beta_0}{2} |\Psi|^4 + \frac{|\mathbf{H}|^2}{8\pi}, \end{aligned} \quad (21)$$

where the \mathbf{x} -dependences are suppressed. While $\alpha(T) = \hbar^2 a(T)/(m_0 c)$ is negative for $T < T_c$ and it changes sign at $T = T_c$, a positive $\beta_0 = \hbar^4 \mathcal{V}_{\text{uc}} b_0/(m_0 c)^2$ (or equivalently b_0) guarantees the energetic stability of the theory. Here \mathcal{V}_{uc} is the volume of the unit cell. In principle m_0 is arbitrary in the GL theory, and physical quantities do not depend on it [31, 33].

In Sec. III B we showed that quantum geometry of the underlying Bloch states has a partial control over those thermodynamic properties that has explicit dependence on the kinetic coefficient c . For instance the London penetration depth $\lambda = \sqrt{m_0 c_0^2/(16\pi q_0^2 |\Psi|^2)}$ is one of them [26, 31, 32], where we substitute $|\Psi|^2 = -\alpha(T)/\beta_0$ assuming weak magnetic fields. This leads to $\lambda(T) = \lambda_{\text{GL}}/\sqrt{\epsilon(T)}$, where

$$\lambda_{\text{GL}} = \sqrt{\frac{\hbar^2 \mathcal{V}_{\text{uc}} b_0}{16\pi m_0 r_0 a_0 c}} \quad (22)$$

is a temperature-independent prefactor. Here $r_0 = q_0^2/(m_0c_0^2)$ is the classical radius of a particle with mass m_0 and charge q_0 in CGS units. Similarly the GL coherence length $\xi(T) = \hbar/\sqrt{2m_0|\alpha(T)|}$ is another example [26, 31, 32], leading to $\xi(T) = \xi_{\text{GL}}/\sqrt{\epsilon(T)}$ where

$$\xi_{\text{GL}} = \sqrt{\frac{c}{2a_0}} \quad (23)$$

is a temperature-independent prefactor. Their ratio $\kappa = \lambda(T)/\xi(T)$ is known as the GL parameter, and it determines whether the superconductor is of type-I or type-II depending on whether $\kappa < 1/\sqrt{2}$ or $\kappa > 1/\sqrt{2}$, respectively. This parameter also depends on quantum geometry through

$$\kappa = \sqrt{\frac{\hbar^2 \mathcal{V}_{\text{uc}} b_0}{8\pi m_0 r_0 c^2}}, \quad (24)$$

and it is independent of temperature. In addition the upper critical field for type-II superconductors $H_{c_2}(T) = \Phi_0/[2\pi\xi^2(T)]$ is another example [26, 31, 32], where $\Phi_0 = \pi\hbar c_0/q_0$ is the superconductivity flux quantum. This leads to $H_{c_2}(T) = H_{c_2}^0\epsilon(T)$, where

$$H_{c_2}^0 = \sqrt{\frac{a_0^2}{m_0 r_0 c^2}} \quad (25)$$

is a temperature-independent prefactor.

Furthermore the superfluid number density $\rho_{\text{sf}}(T)$ can be obtained from the GL free energy of the current-carrying superfluid as follows [34]. Under the assumption of a spatially-uniform condensate, one first imposes the current by applying a phase twist $\Psi(\mathbf{x}) = |\Psi|e^{i\mathbf{q}_{\text{sf}}\cdot\mathbf{x}}$ to the order parameter and reexpress $|\nabla\Psi(\mathbf{x})|^2 = q_{\text{sf}}^2|\Psi|^2$ in Eq. (21), where $\mathbf{v}_{\text{sf}} = \hbar\mathbf{q}_{\text{sf}}/(2m_0)$ is the superfluid velocity associated with the imposed twist. Then $\rho_{\text{sf}}(T)$ is determined from the extra free-energy density $\Delta\mathcal{F} = m_0\rho_{\text{sf}}(T)v_{\text{sf}}^2/2$ of the imposed superfluid flow, where $m_0\rho_{\text{sf}}(T)$ is the so-called superfluid mass density. As a result we identify $\rho_{\text{sf}}(T) = 4|\Psi|^2$, leading to

$$\rho_{\text{sf}}(T) = \frac{4m_0a_0c}{\hbar^2\mathcal{V}_{\text{uc}}b_0}\epsilon(T). \quad (26)$$

Note that Eq. (26) of the GL theory does not coincide with the well-established result that is based on the more appropriate linear-response theory [13], and it may lead to qualitatively accurate but quantitatively inaccurate results in the strong-coupling limit, e.g., see [35] and Sec. III D. Since the phase stiffness $D_{\text{sf}}(T)$ (also known as the helicity modulus or the superfluid weight) is given by $D_{\text{sf}}(T) = \hbar^2\rho_{\text{sf}}(T)/m_0$ [29], the universal Beresinskii-Kosterlitz-Thouless (BKT) relation $T_{\text{BKT}} = \pi D_{\text{sf}}(T_{\text{BKT}})/8$, which determines the superfluid transition temperature in two dimensions, can be written as

$$T_{\text{BKT}} = \frac{\pi a_0 c}{2\mathcal{A}_{\text{uc}} b_0} \epsilon(T_{\text{BKT}}), \quad (27)$$

where \mathcal{A}_{uc} is the area of the unit cell. Thus effective mass of the Cooper pairs, London penetration depth, GL coherence length, GL parameter, upper critical magnetic field, superfluid density and BKT transition temperature are some of those fundamental thermodynamic properties that are partially controlled by the quantum-geometric effects.

D. Application to an isolated flat band

As an application here we consider a weakly-coupled dispersionless flat band that is energetically isolated from the rest of the Bloch bands in the spectrum [12]. Suppose $\varepsilon_{f\mathbf{k}} = \varepsilon_f$ is the energy of this flat band, and it is separated by an energy ε_0 from the nearest band. One can show that $\mu = \varepsilon_f - U(1 - F_f)/(2N_S)$ in the $U/\varepsilon_0 \rightarrow 0$ limit [36], where $0 \leq F_f \leq 2$ is the band filling [37], and we expand $\mathcal{X}_{f\mathbf{k}}/\xi_{f\mathbf{k}} \approx \beta/2 - \beta^2\xi_{f\mathbf{k}}/24 + \dots$ and $\mathcal{Y}_{f\mathbf{k}} \approx 1 - \beta^2\xi_{f\mathbf{k}}^2/4 + \dots$. This leads to $a_0 = 1/(4T_c)$, $b_0 = 1/(48T_c^3)$, $d = [1/(\varepsilon_f - \mu) + i\pi\delta(\varepsilon_f - \mu)]/(8T_c)$, and $c = \frac{1}{4T_c N_c} \sum_{\mathbf{k}} g_0^{f\mathbf{k}}$, where $g_0^{f\mathbf{k}}$ is the isotropic quantum metric of the flat band. See [25] for a comparison with the dispersive-band case. Since d diverges as $\mu \rightarrow \varepsilon_f$ in the $U/\varepsilon_0 \rightarrow 0$ limit, the Cooper pairs have large effective mass, they are weakly repulsive with each other, and their size is small compared to the interparticle spacing. This is because, given that $U/W \gg 1$ with $W \rightarrow 0$ the band width of the flat band, even an arbitrarily small but finite U corresponds effectively to a strong-coupling limit. In addition while the Thouless condition gives $T_c = U/(4N_S)$, Eq. (27) leads to $T_{\text{BKT}} \approx \frac{3\pi U}{8N_S \mathcal{A}} \sum_{\mathbf{k}} g_0^{f\mathbf{k}}$, which is proportional to the inverse-effective mass $\frac{U}{\hbar^2 N_S N_c} \sum_{\mathbf{k}} g_0^{f\mathbf{k}}$ of the two-body bound states [15, 16]. Here $\mathcal{A} = N_c \mathcal{A}_{\text{uc}}$ is the area of the system, and we assumed $T_{\text{BKT}} \ll T_c$. Note that the BKT transition temperature that follows from our simple GL theory almost coincides with the literature, where the prefactor is known to be 1/4 instead of 3/8 at half filling [12]. The root cause of this discrepancy is due to the inaccurate form of Eq. (26) in the strong-coupling limit. Thus, as a result of our GL analysis, we conclude that ξ_{GL} and $H_{c_2}^0$ are independent of U for a flat-band superconductor when $U/\varepsilon_0 \rightarrow 0$, because the ratio $c_{ij}/a_0 = \frac{1}{N_c} \sum_{\mathbf{k}} g_{ij}^{f\mathbf{k}}$ depends only on the average quantum metric over the Brillouin zone.

IV. CONCLUSION

In summary, to gain insight into the thermodynamic properties of multiband superconductors, here we considered a generic multiband Hubbard model, and derived its effective quartic action in the fluctuations of the pairing order parameter near T_c . The effective action is remarkably simple when the system manifests time-reversal symmetry and it exhibits uniform pairing fluc-

tuations in a unit cell at both low momentum and low frequency. In this particular case we derived the TDGL equation, and showed that its kinetic coefficients have a geometric interband contribution that is controlled by both the quantum-metric tensor of the underlying Bloch states and their band-resolved quantum-metric tensors. Through a standard GL analysis, we extracted examples of thermodynamic properties such as the effective mass of the Cooper pairs, London penetration depth, GL coherence length, GL parameter, upper critical magnetic field, superfluid density and BKT transition temperature which have explicit dependence on quantum geometry. Looking ahead our analysis can be extended to

the broken-symmetry state at temperatures $T \ll T_c$ [38], i.e., by again assuming time-reversal symmetry and uniform pairing fluctuations at both low momentum and low frequency. This would verify that the same quantum-geometric terms control the velocity of the Goldstone modes in a completely analogous way [22, 23].

Note added. While finalizing this manuscript, Ref. [39] appeared in the preprint server, where GL theory is derived for an isolated flat band.

ACKNOWLEDGMENTS

The author acknowledges funding from TÜBİTAK.

-
- [1] J. P. Provost and G. Vallee, Riemannian structure on manifolds of quantum states, *Commun. Math. Phys.* **76**, 289 (1980).
- [2] M. V. Berry, Quantal phase factors accompanying adiabatic changes, *Proceedings of the Royal Society of London. A. Mathematical and Physical Sciences* **392**, 45 (1984).
- [3] R. Resta, The insulating state of matter: a geometrical theory, *The European Physical Journal B* **79**, 121 (2011).
- [4] C.-K. Chiu, J. C. Y. Teo, A. P. Schnyder, and S. Ryu, Classification of topological quantum matter with symmetries, *Rev. Mod. Phys.* **88**, 035005 (2016).
- [5] A. Bansil, H. Lin, and T. Das, Colloquium: Topological band theory, *Rev. Mod. Phys.* **88**, 021004 (2016).
- [6] X. Tan, D.-W. Zhang, Z. Yang, J. Chu, Y.-Q. Zhu, D. Li, X. Yang, S. Song, Z. Han, Z. Li, Y. Dong, H.-F. Yu, H. Yan, S.-L. Zhu, and Y. Yu, Experimental measurement of the quantum metric tensor and related topological phase transition with a superconducting qubit, *Phys. Rev. Lett.* **122**, 210401 (2019).
- [7] M. Yu, P. Yang, M. Gong, Q. Cao, Q. Lu, H. Liu, S. Zhang, M. B. Plenio, F. Jelezko, T. Ozawa, *et al.*, Experimental measurement of the quantum geometric tensor using coupled qubits in diamond, *National science review* **7**, 254 (2020).
- [8] A. Gianfrate, O. Bleu, L. Dominici, V. Ardizzone, M. De Giorgi, D. Ballarini, G. Lerario, K. West, L. Pfeiffer, D. Solnyshkov, *et al.*, Measurement of the quantum geometric tensor and of the anomalous Hall drift, *Nature* **578**, 381 (2020).
- [9] H. Tian, X. Gao, Y. Zhang, S. Che, T. Xu, P. Cheung, K. Watanabe, T. Taniguchi, M. Randeria, F. Zhang, *et al.*, Evidence for Dirac flat band superconductivity enabled by quantum geometry, *Nature* **614**, 440 (2023).
- [10] C.-R. Yi, J. Yu, H. Yuan, R.-H. Jiao, Y.-M. Yang, X. Jiang, J.-Y. Zhang, S. Chen, and J.-W. Pan, Extracting the quantum geometric tensor of an optical Raman lattice by Bloch state tomography, (2023), [arXiv:2301.06090](https://arxiv.org/abs/2301.06090).
- [11] P. Törmä, S. Peotta, and B. A. Bernevig, Superconductivity, superfluidity and quantum geometry in twisted multilayer systems, *Nature Reviews Physics* **4**, 528 (2022).
- [12] S. Peotta and P. Törmä, Superfluidity in topologically nontrivial flat bands, *Nature communications* **6**, 1 (2015).
- [13] L. Liang, T. I. Vanhala, S. Peotta, T. Siro, A. Harju, and P. Törmä, Band geometry, Berry curvature, and superfluid weight, *Phys. Rev. B* **95**, 024515 (2017).
- [14] A. Julku, S. Peotta, T. I. Vanhala, D.-H. Kim, and P. Törmä, Geometric origin of superfluidity in the Lieb-lattice flat band, *Phys. Rev. Lett.* **117**, 045303 (2016).
- [15] P. Törmä, L. Liang, and S. Peotta, Quantum metric and effective mass of a two-body bound state in a flat band, *Phys. Rev. B* **98**, 220511 (2018).
- [16] M. Iskin, Two-body problem in a multiband lattice and the role of quantum geometry, *Phys. Rev. A* **103**, 053311 (2021).
- [17] M. Iskin, Effective-mass tensor of the two-body bound states and the quantum-metric tensor of the underlying Bloch states in multiband lattices, *Phys. Rev. A* **105**, 023312 (2022).
- [18] M. Iskin, Exposing the quantum geometry of spin-orbit-coupled Fermi superfluids, *Phys. Rev. A* **97**, 063625 (2018).
- [19] M. Iskin, Quantum-metric contribution to the pair mass in spin-orbit-coupled Fermi superfluids, *Phys. Rev. A* **97**, 033625 (2018).
- [20] K.-E. Huhtinen, J. Herzog-Arbeitman, A. Chew, B. A. Bernevig, and P. Törmä, Revisiting flat band superconductivity: Dependence on minimal quantum metric and band touchings, *Phys. Rev. B* **106**, 014518 (2022).
- [21] J. Herzog-Arbeitman, A. Chew, K.-E. Huhtinen, P. Törmä, and B. A. Bernevig, Many-body superconductivity in topological flat bands (2022), [arXiv:2209.00007](https://arxiv.org/abs/2209.00007).
- [22] M. Iskin, Geometric contribution to the Goldstone mode in spin-orbit coupled Fermi superfluids, *Physica B: Condensed Matter* **592**, 412260 (2020).
- [23] M. Iskin, Collective excitations of a BCS superfluid in the presence of two sublattices, *Phys. Rev. A* **101**, 053631 (2020).
- [24] E. Rossi, Quantum metric and correlated states in two-dimensional systems, *Current Opinion in Solid State and Materials Science* **25**, 100952 (2021).
- [25] C. A. R. Sá de Melo, M. Randeria, and J. R. Engelbrecht, Crossover from BCS to Bose superconductivity: Transition temperature and time-dependent Ginzburg-Landau theory, *Phys. Rev. Lett.* **71**, 3202 (1993).
- [26] S. Stintzing and W. Zwerger, Ginzburg-Landau theory of

- superconductors with short coherence length, *Phys. Rev. B* **56**, 9004 (1997).
- [27] R. O. Umucalilar and M. Iskin, Superfluid transition in the attractive Hofstadter-Hubbard model, *Phys. Rev. A* **94**, 023611 (2016).
- [28] P. Nozieres and S. Schmitt-Rink, Bose condensation in an attractive fermion gas: From weak to strong coupling superconductivity, *J. Low Temp. Phys.* **59**, 195 (1985).
- [29] M. Iskin, Berezinskii-Kosterlitz-Thouless transition in the time-reversal-symmetric Hofstadter-Hubbard model, *Phys. Rev. A* **97**, 013618 (2018).
- [30] According to Ref. [20], the quantum metric is guaranteed to the so-called minimal quantum metric, when the orbitals of the lattice model are fixed by symmetries at high-symmetry points. This symmetry requirement must be equivalent to our condition on uniform pairing fluctuations. For instance inversion symmetry guarantees this in the case of Mielke checkerboard and Kagome lattices [16, 17].
- [31] P. G. de Gennes, Superconductivity of metals and alloys (1966).
- [32] M. Iskin and C. A. R. Sá de Melo, Ultracold fermions in real or fictitious magnetic fields: BCS-BEC evolution and type-I–type-II transition, *Phys. Rev. A* **83**, 045602 (2011).
- [33] A. Leggett, *Quantum Liquids: Bose condensation and Cooper pairing in condensed-matter systems* (Oxford University Press, United Kingdom, 2008) publisher
- Copyright: © Oxford University Press, 2014.
- [34] See also Ref. [33] where the superfluid mass density is derived for a generic GL functional in page 200, or the discussion in Ref. [26].
- [35] For instance Eq. (26) is used in Ref. [26] to calculate T_{BKT} for a two-dimensional continuum Fermi gas with contact interactions. In contrast to the well-established and physically-expected result $T_{\text{BKT}} = 0.125\varepsilon_F$ [40], they found that the BKT transition temperature saturates around $T_{\text{BKT}} \sim 0.11\varepsilon_F$ in the strong-coupling limit, where ε_F is the Fermi energy. This is clearly a qualitatively accurate but a quantitatively inaccurate result.
- [36] M. Iskin, Hofstadter-Hubbard model with opposite magnetic fields: Bardeen-Cooper-Schrieffer pairing and superfluidity in the nearly flat butterfly bands, *Phys. Rev. A* **96**, 043628 (2017).
- [37] When $F_f \rightarrow 0$, we recognize that the binding energy of the lowest bound state is U/N_s in the $U/\varepsilon_0 \rightarrow 0$ limit [16, 17].
- [38] J. R. Engelbrecht, M. Randeria, and C. A. R. Sá de Melo, Bcs to Bose crossover: Broken-symmetry state, *Phys. Rev. B* **55**, 15153 (1997).
- [39] S. A. Chen and K. Law, Towards a Ginzburg-Landau theory of the quantum geometric effect in superconductors, (2023), [arXiv:2303.15504](https://arxiv.org/abs/2303.15504).
- [40] V. M. Loktev, R. M. Quick, and S. G. Sharapov, Phase fluctuations and pseudogap phenomena, *Physics Reports* **349**, 1 (2001).